

Supporting Information

Structures and Conformations of Alkanedithiols on Gold and Silver Nanoparticles in Water

Manuel Gadogbe,[†] Yadong Zhou,[#] Sandamini H. Alahakoon,[†] Ganganath S. Perera,[†] Shengli Zou,[#] Charles U. Pittman Jr.,[†] and Dongmao Zhang^{†}*

[†] Department of Chemistry, Mississippi State University, Mississippi State, Mississippi 39762, United States.

[#] Department of Chemistry, University of Central Florida, Orlando, Florida 32816, United States.

Contents:	Page
S1. UV-vis spectrum and TEM image of the as-synthesized AuNP	S3
S2. Estimation of the monolayer packing concentration of ADT on AuNPs	S4
S3. pH change induced by ADT adsorption onto AuNPs	S5
S4. Computed Raman spectra of intact EDT and EDT monothiolate	S6
S5. Normal Raman spectra of HED/Na ₂ SO ₄ and ME/Na ₂ SO ₄ mixture	S7
S6. Estimation of the Raman cross-section ratio of S-S to S-H for HED and ME	S8
S7. Normal Raman and SERS spectra of ME and HED on AuNPs	S9
S8. Comparison of S/Au ratio for ADT/AuNP and AMT/AuNP aggregates determined by ICP-MS	S10
S9. Time-dependent S-S formation by EDT on AuNPs	S11
S10. Computational modeling of surface plasmon resonance of AuNP aggregates as a function of AuNP gap sizes	S12
S11. TEM images of AgNP/ADT mixtures	S13
S12. TEM images of AuNP/ADT mixtures	S14
S13. Concentration dependence of <i>trans</i> C-S to <i>gauche</i> C-S intensity ratio for ADT on AgNPs	S15
S14. References	S16

S1. UV-vis spectrum and TEM image of the as-synthesized AuNP

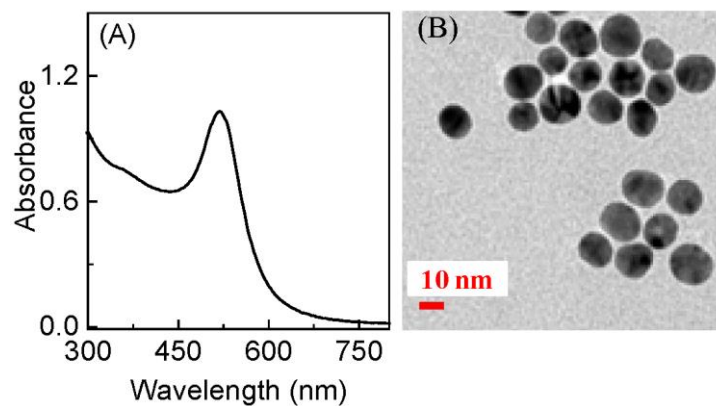


Figure S1. (A) UV-vis spectrum, and (B) an example TEM image of the as-synthesized AuNPs. The scale bar in the TEM image is 10 nm. The UV-vis spectrum is taken with three times diluted sample of the as-synthesized AuNP. The AuNP size was estimated to be $\sim 13 \pm 1.3$ nm from an average size of 56 particles.

S2. Estimation of the monolayer packing concentration of ADT on AuNPs.

The saturation packing density (P in nmol/cm²) of ADT on the AuNP can be expressed as;

$$P = \frac{\Gamma_{\max}}{SA_{\text{total}}} \dots\dots\dots \text{Eq. S1}$$

where Γ_{\max} is the maximum adsorption amount of ADT (nmol) and SA_{total} is the total surface area of the AuNPs in cm².

Assuming the AuNPs are spherical and monodispersed, the surface area for a single AuNP (SA_{AuNP}) can be estimated from the formula;

$$SA_{\text{AuNP}} = \pi D^2 \dots\dots\dots \text{Eq. S2}$$

where D is the AuNP diameter in cm. For the ~13 nm AuNP, SA_{AuNP} was estimated to be 5.31×10^{-12} cm². Using the concentration of the AuNP in the three body mixture (~4 nM) and the Avogadro's number (6.022×10^{23} mol⁻¹), the number of AuNPs in the mixture was calculated to be 7.23×10^{12} particles. SA_{total} is estimated to be 38.39 cm².

Substituting SA_{total} into Eq. S1 and using $P = 0.77$ nmol/cm²,¹ Γ_{\max} is estimated to be 29.54 nmol. The threshold concentration of ADT to form a full monolayer packing capacity on the AuNPs in the three body mixture (3 mL sample) is thus estimated to be ~ 10 μ M.

S3. pH change induced by ADT adsorption onto AuNPs

pH of final washing solution = 6.42

pH of 1 mM BuDT in 50% ethanol (control) = 6.09

Table S1. pH of supernatant of AuNP/BuDT aggregate during BuDT adsorption

Time (min)	pH of supernatant
0 (control)	6.09
5	4.40
15	4.38
30	4.38
1440	4.38

S4. Computed Raman spectra of intact EDT and EDT monothiolate

All the quantum calculations were performed by Gaussian 09 suite. The ground state structures of the EDT were optimized using density functional theory (DFT) method with BP86 functional at the level of 6-311++G (d, p) basis set. Frequency analysis was carried out and no imaginary frequencies were found, ensuring that all of the structures were stable. The Raman spectra were calculated based on these optimized structures using the same functional and basis set as geometry optimization. The calculated wavenumbers in Raman spectra were not scaled by any factor. The Raman intensity ratio of S-H stretch ($\sim 2590\text{ cm}^{-1}$) to C-C stretch ($\sim 1275\text{ cm}^{-1}$) in the computed spectrum reduces from 12 for intact EDT to 3.0 for EDT monothiolate, indicating that the relative Raman activity of the remaining S-H in the EDT monothiolate is only 2 times lower than the average S-H Raman activity in intact EDT. This is in contrast to the 50 times' S-H Raman activity reduction in 1,4-benzenedithiol observed before.²

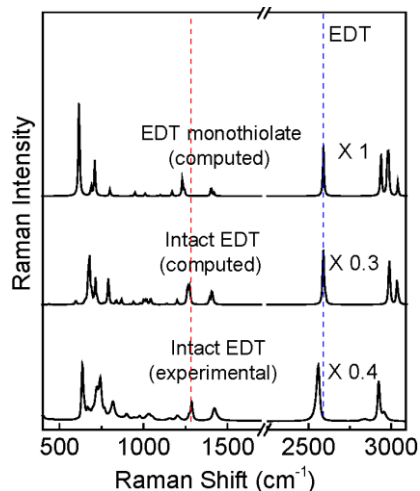


Figure S2. (a) Experimental Normal Raman spectra of intact EDT, and computed Raman spectra of (b) intact EDT and (c) EDT monothiolate. The experimental normal Raman spectrum was acquired with neat EDT. The dotted lines from left to right are the peak positions for C-C stretch (ν_{C-C}) and S-H stretch (ν_{S-H}) respectively

S5. Normal Raman spectra of HED/ Na_2SO_4 and ME/ Na_2SO_4 mixture

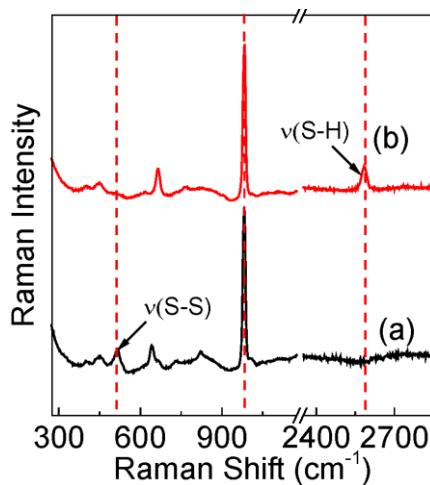


Figure S3. Normal Raman spectra of (a) HED/ Na_2SO_4 and (b) ME/ Na_2SO_4 mixture. Na_2SO_4 was used as internal reference and the peak for SO_4^{2-} at $\sim 983 \text{ cm}^{-1}$ is normalized in both spectra. The nominal concentration of HED and ME in the mixtures is 150 mM. The dotted lines from left to right in the plot represent the peak positions for S-S, SO_4^{2-} , and S-H respectively.

S6. Estimation of the Raman cross-section ratio of S-S to S-H for HED and ME

The Raman cross section ratio $\frac{\sigma_{S-S}^{513}}{\sigma_{S-H}^{2586}}$, between the S-S peak at $\sim 513 \text{ cm}^{-1}$ for HED and the S-H peak at $\sim 2586 \text{ cm}^{-1}$ for ME was estimated by the equation;

$$\frac{\sigma_{S-S}^{513}}{\sigma_{S-H}^{2586}} = \frac{I_{S-S}^{513}}{I_{S-H}^{2586}} \times \frac{C_{ME}}{C_{HED}}$$

Where I_{S-S}^{513} and I_{S-H}^{2586} are the Raman intensities of HED and ME peaks at $\sim 513 \text{ cm}^{-1}$ and $\sim 2586 \text{ cm}^{-1}$ respectively in Figure S2 (a) and (b) respectively. C_{HED} and C_{ME} are the concentrations of HED and ME in the samples mixtures shown in Figure S2 (a) and (b) respectively. The Raman spectra of the sample mixtures were acquired under identical conditions and Na_2SO_4 in both mixtures is the internal reference. The SO_4^{2-} peak in Figure S2 (a) and (b) are normalized. The concentration of HED and ME in the sample mixtures are both 150 mM. On the basis of the Raman spectra shown in Figure S2, the Raman cross section ratio $\frac{\sigma_{S-S}^{513}}{\sigma_{S-H}^{2586}}$ is estimated to be 1.66.

S7. Normal Raman and SERS spectra of ME and HED on AuNPs

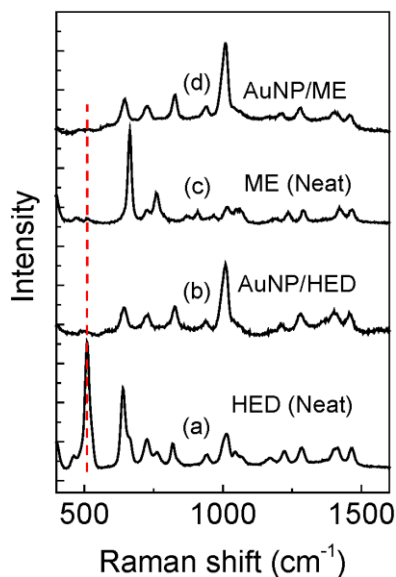


Figure S4. (a, c) Normal Raman spectra of HED and ME respectively, and (b,c) their SERS spectra on AuNPs respectively. The nominal concentration of HED and ME in the SERS samples is 33 μM . The normal Raman spectra were obtained for the neat samples. The dotted line in the plot represents the peak position for S-S. SERS results show that HED adsorbs dissociatively through breaking of the S-S bond as evidenced by the close resemblance of the AuNP/ME and AuNP/HED SERS spectra.

S8. Comparison of S/Au ratio for ADT/AuNP and AMT/AuNP aggregates determined by ICP-MS

Table S2. Comparison of S/Au ratio of BuT/AuNP, EDT/AuNP, BuDT/AuNP, and HDT/AuNP determined using ICP-MS.

Sample	S/Au	S/Au / (S/Au) _{BuT}
AuNP/BuT	0.05 ± 0.001	1 ± 0.03
AuNP/EDT	0.05 ± 0.007	1 ± 0.1
AuNP/BuDT	0.04 ± 0.004	0.8 ± 0.1
AuNP/HDT	0.03 ± 0.001	0.6 ± 0.02

S9. Time-dependent S-S formation by EDT on AuNPs

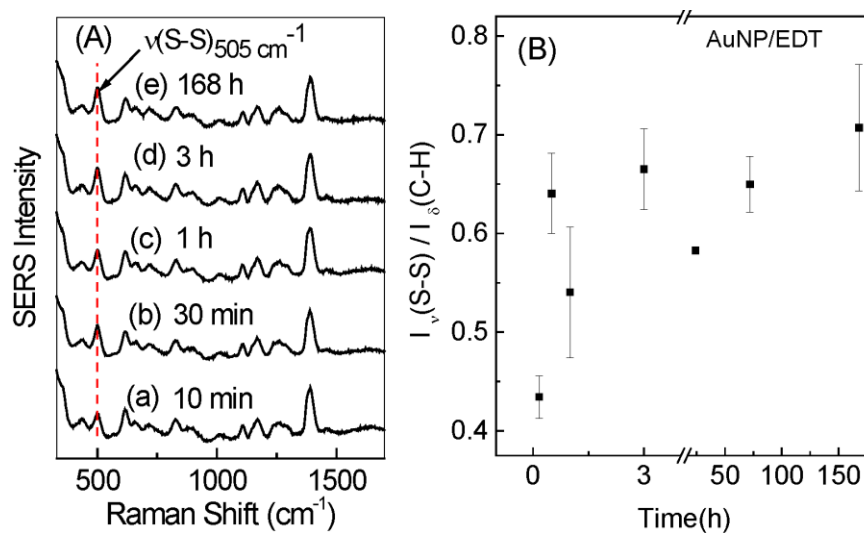


Figure S5. (A) Time dependent SERS spectra of AuNP/EDT. (B) Plot of the intensity ratio of S-S to C-H bending as a function of time. The nominal concentration of EDT in the samples is 10 μM .

S10. Computational modeling of surface plasmon resonance of AuNP aggregates as a function of AuNP gap sizes.

The T-matrix method was used to calculate the extinction spectra of AuNP aggregates with different spacing between AuNPs.³ In the calculations, the coordinates of the AuNPs were generated using Monte Carlo method. The first particle was placed at the origin of the coordinate, the following particle coordinates are generated using Monte Carlo method and their distance with the previous particles are kept above a fixed minimum value. For example, if the minimum distance was fixed at 1.4 nm, the distance between the first and the second particle is 1.4 nm, the distance between n th and $(n+1)$ th particles is also kept at 1.4 nm, however, the distances between $(n+1)$ th particle with all other particles are always over 1.4 nm so that the generated aggregate is similar to the experimentally generated amorphous structure. Once the coordinates of particles were generated, their interaction and extinction spectra were calculated using T-matrix method. In the simulations, the distance was varied from 1.4 nm to 4.28 nm, as shown in Figure S6, the resonance wavelength shifts to blue with increasing minimum interparticle distance. In the experiments, the diameter of the particles is 13 nm, over several thousands of particles were required to simulate the comparable size of the aggregate which is not affordable using our computer resource. We used particles with diameter of 50 nm to show the trend in the spectra change when the interparticle distance is changed. Only 50 particles are required to generate extinction spectra with resonance wavelength ranging from 700-800 nm. As shown in Figure S6, the calculated extinction spectra qualitatively agree with the experimentally measured spectra.

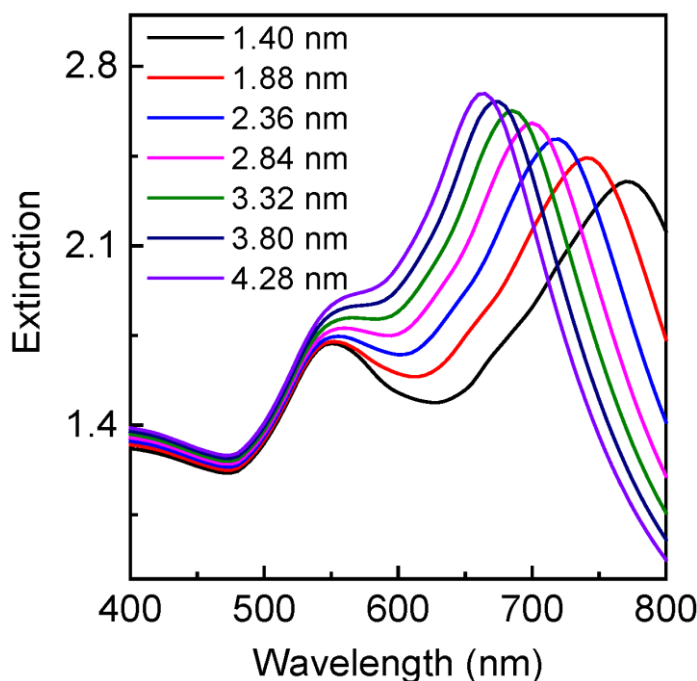


Figure S6. Computational simulation for the LSPR shift of AuNP aggregates as a function of the AuNP gap sizes. The particle diameter of AuNP is 50 nm and the total number of AuNPs is 50.

S11. TEM images of AgNP/ADT mixtures

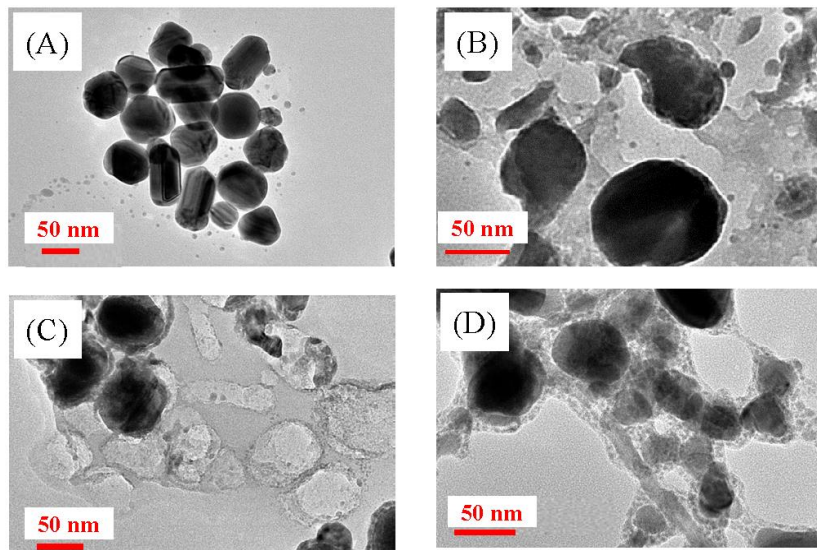


Figure S7. TEM images of (A) AgNP, (B) AgNP/EDT, (C) AgNP/BuDT, and (D) AgNP/HDT. The samples were prepared by mixing 1 mL of two times diluted AgNP with 1 mL water followed by 1 mL of the ADT. The concentration of ADT in the TEM samples is 33 μ M. The TEM images were taken after 4 days of sample incubation.

S12. TEM images of AuNP/ADT mixtures

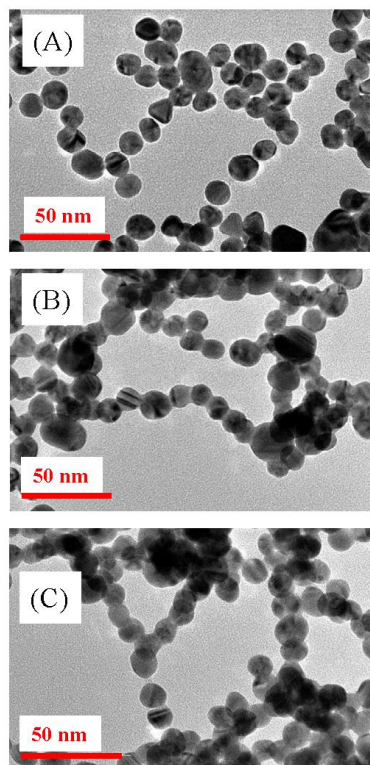


Figure S8. TEM images of (A) AuNP/EDT, (B) AuNP/BuDT, and (C) AuNP/HDT. The samples were prepared by mixing 1 mL of AuNP with 1 mL water followed by 1 mL of the ADT. The concentration of ADT in the TEM samples is 33 μM . The TEM images were taken after 4 days of sample incubation.

S13. Concentration dependence of *trans* C-S to *gauche* C-S intensity ratio for ADT on AgNPs

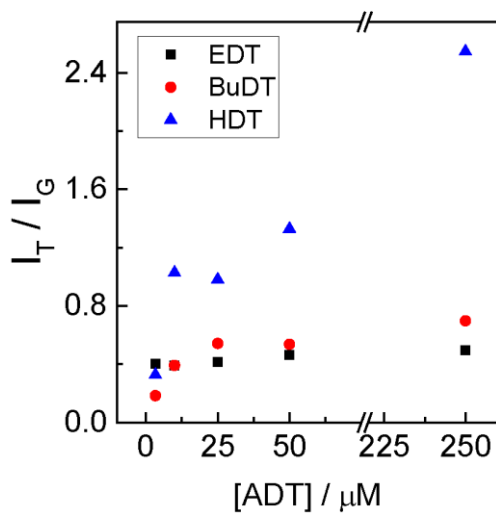


Figure S9. Intensity ratio of C-S *trans* to C-S *gauche* as a function of the nominal ADT concentration. The ratio is determined from the SERS spectra of ADT on AgNPs.

S14. References

1. Weisbecker, C. S.; Merritt, M. V.; Whitesides, G. M., Molecular Self-Assembly of Aliphatic Thiols on Gold Colloids. *Langmuir* **1996**, *12*, 3763-3772.
2. Gadogbe, M.; Chen, M.; Zhao, X.; Saebo, S.; Beard, D. J.; Zhang, D., Can Para-Aryl-Dithiols Cross-Link Two Plasmonic Noble Nanoparticles as Monolayer Dithiolate Spacers? *J. Phys. Chem. C* **2015**, *119*, 6626-6633.
3. Mishchenko, M. I.; Travis, L. D.; Mackowski, D. W., T-matrix computations of light scattering by nonspherical particles: A review. *J. Quant. Spectrosc. Radiat. Transfer*. **1996**, *55*, 535-575.